

N94-22746

SAW Based Systems for Mobile Communications Satellites

R.C. Peach, N. Miller and M. Lee

COM DEV Ltd.
155 Sheldon Drive
Cambridge, Ontario
N1R 7H6
(519) 622-2300
(519) 622-1691**ABSTRACT**

Modern mobile communications satellites, such as INMARSAT 3, EMS and ARTEMIS, use advanced on-board processing to make efficient use of the available L-band spectrum. In all of these cases, high performance surface acoustic wave (SAW) devices are used. SAW filters can provide high selectivity (100-200 kHz transition widths), combined with flat amplitude and linear phase characteristics; their simple construction and radiation hardness also makes them especially suitable for space applications.

This paper gives an overview of the architectures used in the above systems, describing the technologies employed, and the use of bandwidth switchable SAW filtering (BSSF). The tradeoffs to be considered when specifying a SAW based system are analyzed, using both theoretical and experimental data. Empirical rules for estimating SAW filter performance are given. Achievable performance is illustrated using data from the INMARSAT 3 engineering model (EM) processors.

1.0 INTRODUCTION

All L-band mobile communication systems must operate within 34 MHz spectrum allocations (1525-1559 MHz forward link, 1626.5-1660.5 MHz return link), and must be able to service low gain mobile terminals. To cope with these limitations, systems such as INMARSAT 3, EMS and ARTEMIS use multiple spot beams, frequency re-use, and flexible frequency allocation between beams.

These systems require complex on-board processors, which use combinations of splitters, amplifiers, SAW filters and switch matrices to route traffic to the appropriate beams. Of these processors, which are currently under development at COM DEV, INMARSAT is by far the most sophisticated, though ARTEMIS has the most selective filters. The INMARSAT system also makes limited use of a technique called bandwidth switchable SAW filtering

(BSSF), or seamless combining, which allows a significant recovery of guard band spectrum [1] [2]. The principle of this method is to use banks of contiguous filters with the special property that adjacent filters, when operated simultaneously, add to form a continuous response without distortion in the crossover (guard band) region. Therefore, when a group of adjacent filters are allocated to a single beam, the entire band covered by the filters is usable, without any loss to intermediate guard bands.

An overview of SAW based processor architectures is given in section 2.0 of this paper, and the tradeoffs associated with the SAW filters are discussed in Section 3.0.

2.0 SYSTEM ARCHITECTURES

Figure 1 shows a simplified schematic of the INMARSAT 3 forward processor, proposed by Matra Marconi Space (MMS) and built by COM DEV, while Figure 2 shows an exploded view of its physical realization. The return processor is essentially similar, except for the reversal of the signal paths, and the addition of programmable gain in the individual filter channels.

The key parameters for the INMARSAT 3 processor are:

- Channel bandwidths from 4.5 to 0.45 MHz
- 20 dB Noise Figure
- Intermodulation products <-45 dBc
- 35 dB Nominal gain
- 40 dB of programmable gain
- Maximum mass 35 Kg (total of forward and return processors)
- Maximum power consumption 100 W (total of forward and return processors)
- High spectral efficiency (200 kHz guard bands, BSSF)

Dual redundant right and left circularly polarized (RHCP and LHCP) L-band input signals are split between a total of 15 filter modules, where they are down converted to a 160 MHz IF. Each filter module contains SAW filterbanks to channelize the spectrum, followed by GaAs FET switch matrices which allow any filter output to be routed to any one of eight output beams. The signals are upconverted to the final L-band frequency before leaving the filter modules, and are then combined in the eight output modules (one per beam). The mechanical arrangement is forced by the signal splitting and combining requirements. The input, output and LO distribution modules are housed in the horizontal stack, and interface with the filter modules in the vertical stack by blind mate connectors; this allows full connectivity between any input or output module and any filter module. Telecommand and telemetry is handled by the control module, which is placed on top of the vertical (filter) modules; control signals are routed to the horizontal modules via an additional housing on the side of the processor. To minimize mass, all module housings are machined from magnesium.

The input modules are among the simplest in the system. They contain redundant thin film GaAs input amplifiers and eight way power dividers implemented with cascaded Wilkinson splitters on high dielectric soft substrates. The output modules perform an inverse function, but are considerably more complex. In addition to combiners and amplifiers, they contain programmable gain blocks implemented with GaAs FET switches and controlled by an ASIC; interdigital bandpass filters are used to remove mixer spurious.

The filter modules, shown schematically in Figure 3, are the key elements in the system, as these provide all the frequency selectivity and signal routing. Three main types of filter module are employed, which differ in the frequency and bandwidth of their SAW filters, though a guard bandwidth of 200 kHz is used throughout. Each non-redundant module has a specific LO frequency that determines its position in the 34 MHz frequency band. Redundant modules can use any LO frequency, and can therefore substitute for any module of similar type. The implementation of the INMARSAT frequency plan with only three module types is another example of the use of BSSF. Because of the contiguous combining, a given filter bank can realize several channelization schemes, allowing greater standardization of module types, and hence greater reliability.

For reasons discussed in Section 3.0, the SAW Filters must operate at a relatively low IF; 160 MHz was

chosen as a compromise between minimizing operating frequency and minimizing fractional bandwidth. After down conversion, the IF signals are amplified by discrete bipolar amplifiers optimized for low power consumption. The signals are then applied to the inputs of the two SAW filterbanks, each of which may contain up to three channels. Each filterbank output is then amplified by discrete amplifiers and fed into a 3x9 switch matrix, which allows any channel to be switched to any beam, or to be terminated if not in use. The switch matrix uses surface mount construction, and is built from custom hybridized units each containing three single pole double throw (SPDT) GaAs FET switches and a three way resistive power combiner. Isolation between channels is typically 60 dB. An ASIC controls the switch matrix operation. After routing through the switch matrix, each of the eight outputs is upconverted to L-Band. The up conversion frequency is offset from the down conversion frequency to minimize spurious signals.

The LO frequencies are generated externally to the processor and are distributed by the LO module. This uses combinations of power splitters and GaAs FET switches to route the LO signals to the appropriate filter modules. However, the distribution requirements are extremely complex, and the LO module is correspondingly complex.

The EMS system is far simpler in concept than INMARSAT, though similar technologies are used. It is being built by COM DEV and AME Space for Alenia Spazio as a supplementary payload for ITALSAT 2. The schematic of the EMS forward processor is shown in Figure 4. A Ku band uplink is employed, rather than the C-band uplink used for INMARSAT. Three 4 MHz wide slots are selected and down converted to an IF of approximately 145 MHz, where they are channelized by a non-contiguous bank of SAW filters with 250 kHz transition widths. The outputs are then upconverted to the L-band channels 1530-1534 MHz, 1540-1544 MHz and 1555-1559 MHz, using different LOs for each filter.

The EMS return processor replaces each 4 MHz filter with a bank of four 900 kHz filters, each with independent programmable gain. Selective use of these subchannels allows coordination with other systems using the same frequency bands. The return filters have centre frequency separations of 1 MHz and transition widths of 200 kHz; BSSF is not employed. This frequency plan produces overlap between filters, and hence a reduction in the usable filter bandwidth when adjacent filters are operated simultaneously. The ARTEMIS system is very similar to EMS, but the return

filter transition width is reduced to 100 kHz to avoid overlap. No attempt is made to recover these remaining 100 kHz guard bands using BSSF, but this would be a logical extension for future systems.

3.0 SAW FILTER TECHNOLOGY FOR ON-BOARD PROCESSING

SAW filters are particularly well suited to the high selectivity, linear phase requirements in on-board processing. However their characteristics are very different from those of classical filters, and this often causes confusion when systems are specified. This section discusses the tradeoffs and limitations associated with this class of SAW filter, based on both theoretical and empirical data.

Reference [1] discusses the basic properties of SAW filters for mobile communication systems, including BSSF. The SAW transversal filters used in INMARSAT, EMS and ARTEMIS, all use in-line transducer structures [1]. The transducers contain numerous interdigitated electrodes (typically 3000 to 9000), formed by photolithography in a thin (1000-2000Å) aluminium film deposited on the polished surface of a piezoelectric crystal; ST-X quartz is used for these systems on account of its temperature stability. Each transducer has an ideal frequency response similar to that of a finite impulse response (FIR) digital filter; the electrodes serve as the taps, and their weights are controlled by varying the overlaps (apodization). The SAW propagation time between electrodes is equivalent to the sampling time.

The transfer functions of SAW transversal (or FIR) filters have no poles in the finite s plane, only zeros. They are usually also of very high order compared to classical filters (10000 electrodes in a transducer is not uncommon). Design techniques are therefore quite different, and are usually based on optimization techniques. Of these, linear programming [1] offers unrivalled flexibility. Current programs based on linear programming can design both filters and filterbanks with arbitrarily specified amplitude and phase responses. The most common requirement is for linear phase, flat amplitude characteristics, both for the individual and the combined filter responses.

For SAW filters, impulse response length is the most appropriate measure of filter complexity. For a linear phase design, a simple empirical rule can be used to predict the impulse response length [3].

$$\log(\delta_p \delta_s) = -1.05 - 1.45 BT \quad (1)$$

where B = transition bandwidth from passband to stopband edge.

T = impulse response length
 $20\log((1+\delta_p)/(1-\delta_p))$ = Passband ripple (dB)

$20\log(\delta_s)$ = Stopband level (dB)

In the great majority of designs T is 2-3 times the reciprocal of B . It should also be noted that T is determined by the transition width, and is virtually independent of absolute bandwidth; it is also independent of centre frequency. The physical size of the filter can be obtained by multiplying T by the SAW velocity. However, the final size is significantly greater than this estimate for two reasons: first, the response must be factored between the two transducers in a non-optimal way, and second, a reasonable separation must be allowed between transducers to avoid electromagnetic coupling.

The choice of factorization is forced by practical considerations. For an in-line transducer structure the allowable weighting pattern on one transducer is restricted so that each electrode covers either all or none of the aperture (withdrawal weighting). Without this, the overall response would not, even to first order, be the product of the individual transducer responses, and this defeats all existing synthesis procedures. Empirically, it is well established that individual transducers rarely provide more than 35 dB of close-in rejection. To achieve higher rejections than this both transducers must contribute significantly to the out of band response. The withdrawal weighted transducer is therefore chosen to have reasonable out of band rejection and a reasonably regular passband response. The apodized transducer can then be designed to satisfy the overall specification. The design is then optimized to correct for second order effects, such as SAW diffraction and circuit loading, but corrections are applied to the apodized transducer alone, the other transducer is left fixed; this procedure is most effective if the length of the withdrawal weighted transducer is minimized. These design constraints are incompatible with fully optimal factorization, and some length penalty must be accepted. In addition, the requirements of BSSF and of correcting for second order effects also produce a length penalty.

For INMARSAT 3 the specified transition bandwidth is 200 kHz for all filters. However, a design value of 170 kHz was used, allowing 10 kHz margin for temperature drift and ± 10 kHz for manufacturing tolerances. With design passband ripples and stopband

levels of 0.2 dB and 50 dB respectively, equation (1) predicts an impulse response length of 13.70 μ s, equivalent to 4.34 cm for quartz (SAW velocity 3159 m/s). The actual length is approximately 7.1 cm, including 0.9 cm spacing between transducers. The net effect of all the above constraints is therefore to increase the total transducer length by about 40% from the estimate given by equation (1).

A 100 kHz transition width is specified for the ARTEMIS return filters, and a 75 kHz value has been used in the design. Combined with a 0.25 dB passband ripple and a 50 dB stopband level, equation (1) gives a predicted impulse duration of 30.3 μ s (9.56 cm on quartz). The length of the final design is 12.6 cm including 1 cm transducer separation. The net transducer length is therefore 21% greater than the ideal limit. This difference between the ARTEMIS and INMARSAT filters reflects the absence of BSSF constraints, and the use of a more sophisticated factorization procedure for the ARTEMIS designs. A reasonable practical estimate of overall filter length can therefore be obtained by taking the value of T from equation (1), increasing this by 30%, multiplying by the SAW velocity, and adding the transducer separation (0.5-1.0 cm) and an allowance for packaging (0.5-1 cm).

Manufacturing sensitivity is a critical factor in determining the minimum transition bandwidth and maximum operating frequency of a SAW filter. Photolithographic capabilities will allow operation at 1 GHz and above, but the achievable filter performance is severely degraded, and high selectivity, high precision filters are restricted to comparatively low frequencies. The major limiting factors are:

- Metallization uniformity
- Electrode linewidth control
- Photomask aberrations
- Substrate uniformity
- Substrate mounting stresses

All of these produce similar effects, which may be modelled as a variation in SAW propagation velocity. If such velocity errors are random, and average out over a short distance scale, they are comparatively harmless. However, the above effects usually produce troublesome long range variations.

For a given effective velocity error, the filter distortion is directly proportional to centre frequency. If the peak to peak velocity variations are similar for different filter lengths, then the distortion is also inversely proportional to the transition bandwidth. In addition, the velocity

perturbation caused by the metallisation increases in proportion to frequency. Unfortunately, there is no precise model available for assessing all tradeoffs; however, the following empirical formulas give a reasonable estimate of the achievable P-P passband ripples for an individual high selectivity quartz filter:

$$\text{P-P amplitude ripple} = \text{Design ripple} + 15tF^2/B \text{ dB} \quad (2)$$

$$\text{P-P phase ripple} = \text{Design ripple} + 250tF^2/B \text{ deg} \quad (3)$$

where t = metallization thickness (m) (typically 1e-7 to 2e-7 m)
 F = centre frequency (MHz)
 B = transition bandwidth (MHz)

The centre frequency should therefore be kept as low as possible, compatible with the fractional bandwidth constraints for the material; for filters with transition widths less than 200 kHz, 200 MHz is a reasonable upper limit.

So far, the effect of shape factor (ratio of bandwidth at stopband edges to bandwidth at passband edges) has not been considered; it does not directly affect device size but it does have a slight effect on passband ripple and out of band rejection. A low shape factor (very square response) is more difficult to realize with a withdrawal weighted transducer, and the overall filter rejection is reduced as a result. For shape factors of 1.2 or greater, close in rejections of 50 dB and far out rejections of 60 dB are achievable. For shape factors of 1.1, these values are reduced to 45 dB and 50 dB respectively. Achievable rejection is also weakly dependent on centre frequency.

4.0 EXPERIMENTAL SYSTEM PERFORMANCE

Figure 6 shows the combined response of two L-band channels measured on the INMARSAT EM forward processor shown in Figure 5. The individual filters have bandwidths of 0.75 MHz and 2.11 MHz, and together with a 0.54 MHz device form a contiguous set of three filters; including the guard band they give a total bandwidth of 3.06 MHz. Figure 7 shows the response of the 2.11 MHz filter combined with its other neighbouring filter to give a net bandwidth of 2.85 MHz. This demonstrates that BSSF can provide characteristics that are virtually indistinguishable from those of individual filters. In the above measurements the unused channels were switched to other outputs (beams); the absence of any residual responses

demonstrates the low levels of leakage in the SAW package, the switch matrix, and the splitter driving the output mixers.

Figures 8 and 9 show the combined in-band amplitude and phase responses of the three filters. The overall amplitude ripple is approximately 0.5 dB P-P. Although not observable in this case, some crossover distortion usually arises, and the ripple in the crossovers is often a few tenths of a dB worse than in other regions. The phase ripple clearly shows the transitions between the individual filters. This ripple could be improved by further alignment; but this is not justified as the phase requirements are comparatively non-critical. The filters are all made in matched sets and little change is observed in passband characteristics over the operating temperature range (-15 to 75°C).

5.0 CONCLUSIONS

The development of the INMARSAT and EMS systems has clearly demonstrated the feasibility of using SAW based on-board processors for spectrum allocation and routing. It has also provided a great deal of valuable information about the tradeoffs associated with the various technologies, particularly the SAW filters.

The greatest technical challenges have not been associated with individual components, but rather with the integration of so many technologies into a complete system. Other difficulties have only become fully evident during system level testing. Particularly notable in this regard is the control of spurious signals. The large number of signals and LOs going into the processors, and the large number of leakage paths and non-linear components, make spurious generation a major problem; work is still in progress to isolate and suppress unwanted signals.

ACKNOWLEDGEMENTS

The authors would like to acknowledge the invaluable contributions of P. Kenyon, R. Kovac, B. Van Osch and A. Veenstra to this work.

6.0 REFERENCES

[1] R. Peach & A. Malarky, "Enhanced Efficiency using Bandwidth switchable SAW Filtering for Mobile Satellite Communications Systems", *Proc. IMSC*, pp394-402, 1990.

[2] O. Andreassen, "A SAW Filter Bank for Telecommunications applications", *Microwave and RF Engineering*, pp43-48, Jan/Feb 1990.

[3] D.P. Morgan, "Surface-Wave Devices for Signal Processing", *Amsterdam: Elsevier*, 1985.

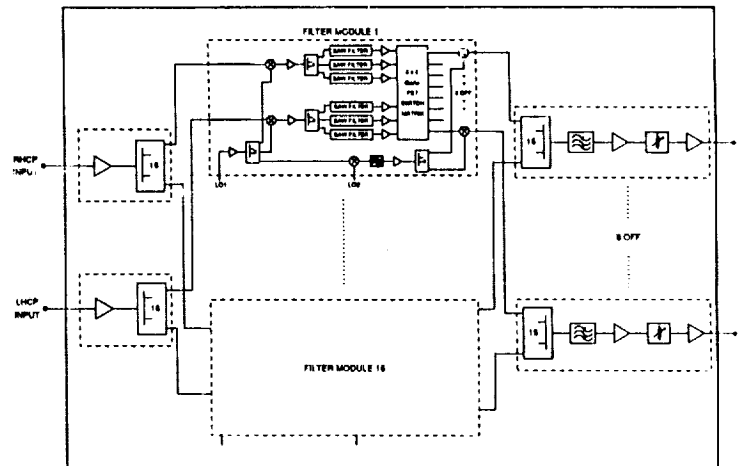


Figure 1. Simplified schematic of INMARSAT 3 forward processor

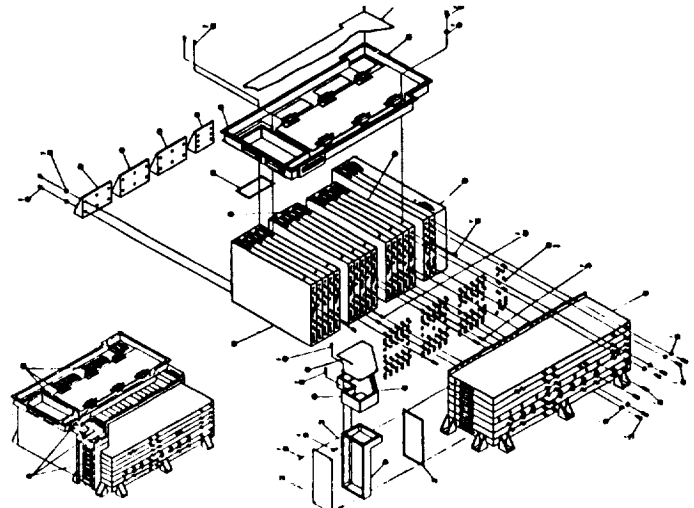


Figure 2. INMARSAT 3 forward processor construction

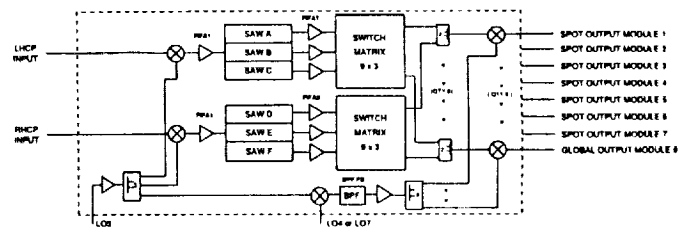


Figure 3. Simplified schematic of INMARSAT filter module

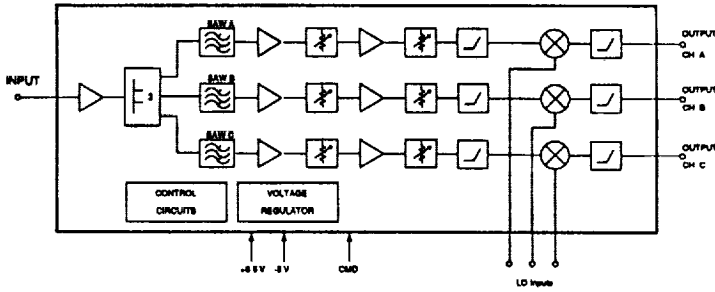


Figure 4: Schematic of EMS filter module

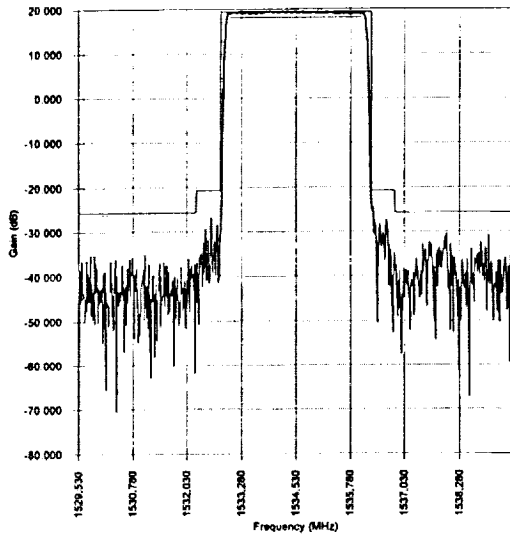


Figure 6. Combined frequency response of channels D and E

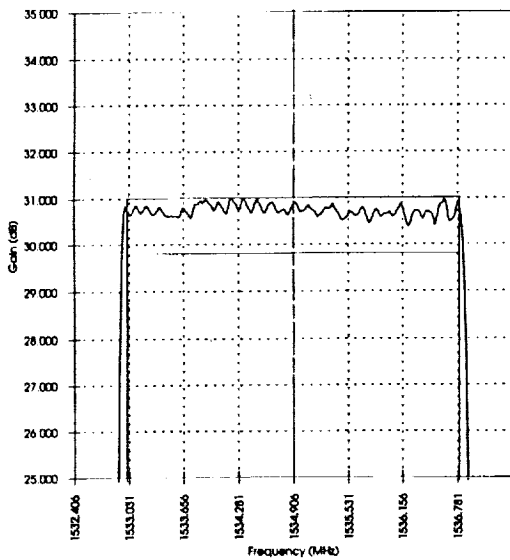


Figure 8. Combined amplitude response of channels D, E and F

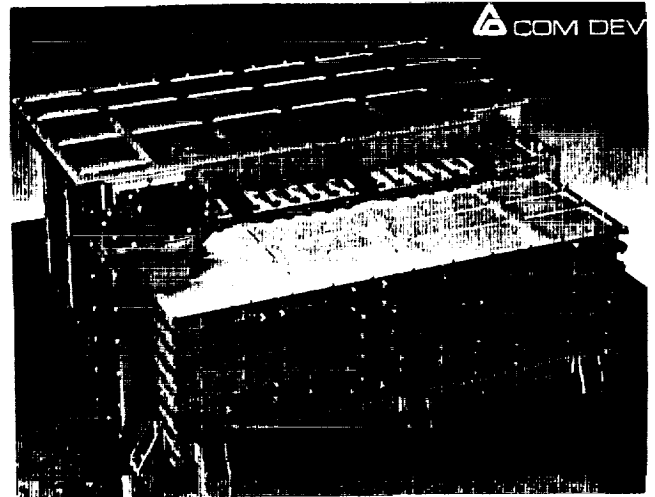


Figure 5. INMARSAT 3 EM forward processor

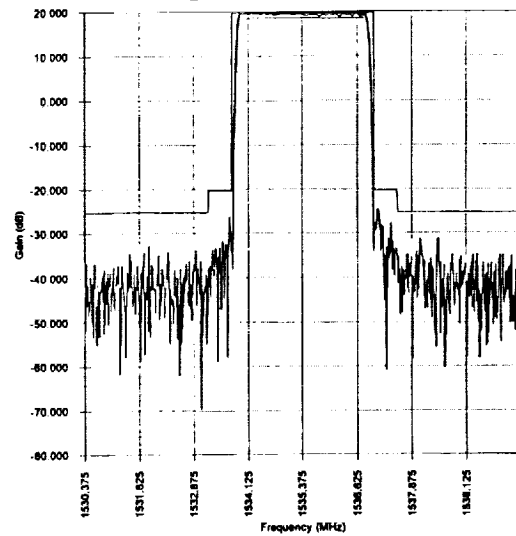


Figure 7. Combined frequency response of channels E and F

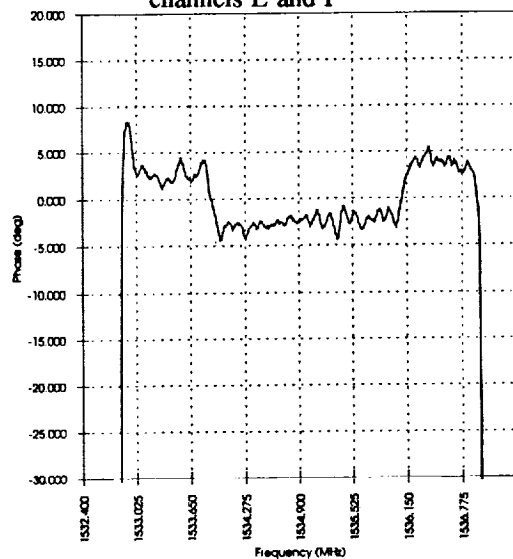


Figure 9. Combined phase response of channels D, E and F